Arch. Metall. Mater. **65** (2020), 4, 1293-1296

DOI: 10.24425/amm.2020.133687

JU-YOUNG CHO[1,2], YONG-HO-CHOA[2], SUN-WOO-NAM[1],
RASHEED MOHAMMAD ZARAR[1,3], TAEK-SOO KIM[1,3*]

EFFECT OF TEMPERATURE ON THE PLASTIC DEFORMABILITY OF GAS ATOMIZED NdFeB ANISOTROPIC MAGNETS

NdFeB anisotropic sintered permanent magnets are typically fabricated by strip casting or melt spinning. In this study, the plastic deformability of an NdFeB alloy was investigated to study the possibility of fabricating anisotropic sintered magnets using gas atomized powders. The results show that the stoichiometric composition $Nd_{12}Fe_{82}B_6$ softens at high temperatures. The aspect ratio and orientation factor of $Nd_{12}Fe_{82}B_6$ billets after plastic deformation were found to increase with increasing plastic deformation temperature, particularly above 800°C. This confirms that softening at high temperatures can lead to plastic deformation of $Nd_2Fe_{14}B$ hard magnetic phases.

Keywords: NdFeB permanent magnet, stoichiometric composition, gas atomization, plastic deformability, crystal orientation

1. Introduction

NdFeB anisotropic sintered magnets are in high demand in fields, such as electric vehicles, wind generators, magnetic resonance imaging, and factory automation systems, owing to their excellent magnetic properties. NdFeB magnets are generally fabricated using two sintering methods, one of which involves employing pulverized powder obtained from casted strips by a combination of hydrogen decrepitation (HD) and jet milling. In the other method, hot deformation is performed by die-upsetting pulverized melt-spun ribbons [1-3].

Although the gas atomization technique has been used to produce metal powders, it has rarely been applied to the fabrication of NdFeB anisotropic sintered magnets; this is because it results in poor magnetic properties, as the grain size of a gas atomized powder is greater than those of traditional powders, and the texture is random [4-6]. However, if NdFeB anisotropic sintered magnets of industrial grade can be fabricated using gas atomized powders, conventional methods can be replaced, as it can not only simplify the process but can also prevent oxidization of NdFeB alloy.

To this end, alignment with the c-axis, which is the easy magnetization axis of NdFeB magnets, has been studied using atomized powders through plastic deformation [5-7]. However, the plastic deformation process of NdFeB magnets fabricated using gas atomized powders has some limitations. First, an NdFeB magnet mainly contains $Nd_2Fe_{14}B$ and Nd-rich phases, with the $Nd_2Fe_{14}B$ hard magnetic phase having only two slip systems at room temperature [8]. Therefore, the deformation must occur at high temperatures. The second limitation is the presence of the Nd-rich phase, which acts as a decoupling agent between the hard magnetic phases and has a low melting point of approximately 660°C. This makes it a deformation inhibitor of hard magnetic phases above 660°C [9].

The aim of this study was to investigate the plastic deformability of the $Nd_2Fe_{14}B$ hard magnetic phase obtained through a gas atomized powder. The Nd composition was controlled to increase the possibility of plastic deformation at high temperatures, the effect of which was investigated through high-temperature Vickers hardness testing at various compositions. In addition, the microstructure and c-axis alignment were investigated with respect to the plastic deformation temperature.

2. Experimental

$Nd_{15.22}Fe_{78.63}B_{6.15}$ and $Nd_{12}Fe_{82}B_6$ compositions were prepared to investigate the softening of the $Nd_2Fe_{14}B$ hard magnetic

[1] KOREA INSTITUTE FOR RARE METALS, KOREA INSTITUTE OF INDUSTRIAL TECHNOLOGY, GAETBEOL-RO 12, SONGDO-DONG, INCHEON 21999, KOREA
[2] HANYANG UNIVERSITY, DEPARTMENT OF MATERIAL SCIENCE AND CHEMICAL ENGINEERING, ANSAN, KOREA
[3] UNIVERSITY OF SCIENCE AND TECHNOLOGY,CRITICAL MATERIALS AND SEMI-CONDUCTOR PACKAGING ENGINEERING, DAEJEON 3413, REPUBLIC OF KOREA

* Corresponding author: tskim@kitech.re.kr

phase. The alloys were prepared by induction melting in an alumina crucible, followed by gas atomization (Model: DTIH-0050MF, Dongyang Induction Melting Furnace Corporation, Korea) at 1500°C under a gas pressure of 40 bar. The atomized powder was sieved; the powder size was in the range of 25-38 μm. The gas-atomized $Nd_{15.22}Fe_{78.63}B_{6.15}$ and $Nd_{12}Fe_{82}B_6$ compositions were pre-compacted at 750°C under a pressure of 20 MPa in a 12Φ graphite mold, and the hardness was measured using a high-temperature Vickers hardness tester (Model: AVK-HF, Mitutoyo) at temperatures ranging from 100 to 900°C at intervals of 100°C. The pre-compacted $Nd_{12}Fe_{82}B_6$ billets were plastic deformed by varying the temperature from 700 to 900°C after every 100°C under a pressure of 50 MPa in a 22Φ graphite mold using spark plasma sintering (SPS) equipment (Model: SPS-20, Welltech Co., Korea). The microstructures of the powder, pre-compacted billets, and plastic-deformed billets were observed using field emission scanning electron microscopy (FE-SEM) (Model: JSM-7100F, JEOL). The aspect ratio of the powder was calculated using an image analyzer (Image J software). To investigate the degree of c-axis alignment, the diffraction peak was observed using X-ray diffraction (XRD) (Model: D8 Advance, Bruker), and the orientation factor was calculated with respect to the plastic deformation temperature.

3. Results and discussion

Fig. 1 shows the Vickers hardness values of $Nd_{15.22}Fe_{78.63}B_{6.15}$ and $Nd_{12}Fe_{82}B_6$ with respect to temperature. The hardness of $Nd_{15.22}Fe_{78.63}B_{6.15}$ decreases from 595 to 550 as the temperature increases from 100 to 600°C. The hardness value above 600°C could not be measured because of the melting of the Nd-rich phase. To overcome this problem, billets of the stoichiometric composition $Nd_{12}Fe_{82}B_6$ were prepared by SPS of the gas atomized powder to confirm the hardness value of the $Nd_2Fe_{14}B$ phase without the Nd-rich phase. The Vickers hardness value was found to decrease from HV 643 to HV 150 with an increase in temperature from 100 to 900°C. In particular, the hardness decreased significantly above 800°C, suggesting a rapid softening of the $Nd_2Fe_{14}B$ phase above 800°C.

According to the results of the hardness test, the powder fabricated by gas atomization was composed of $Nd_{12}Fe_{82}B_6$, and

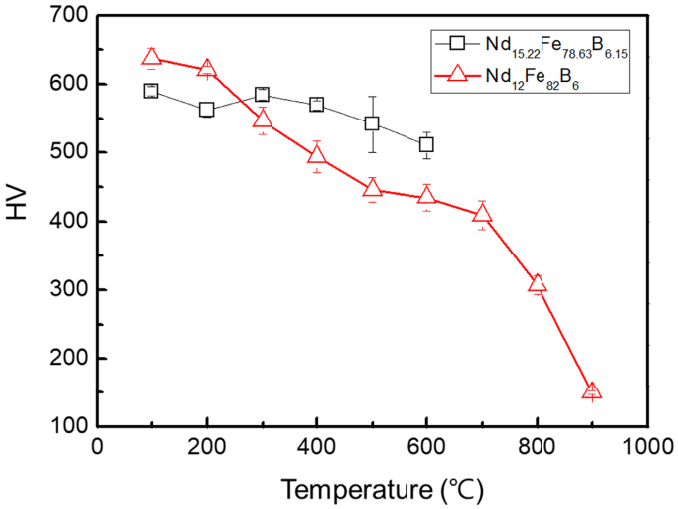

Fig. 1. Vickers hardness values of $Nd_{15.22}Fe_{78.63}B_{6.15}$ and $Nd_{12}Fe_{82}B_6$ compositions with temperature

as predicted elsewhere [9], it exhibited poor magnetic properties. Since the purpose here was to confirm the plastic deformability of the $Nd_2Fe_{14}B$ phase, the poor magnetic properties of the fabricated sample were considered insignificant. Figs. 2(a)-(c) show the cross sections of the microstructures of the atomized powders. As shown in Fig. 2, the atomized powders consist of α-Fe (dark), $Nd_2Fe_{14}B$ (gray) and Nd-rich (white) phases, with α-Fe phase fractions of 0, 4.69, and 18.94% corresponding to powder sizes of 10, 40, and 70 μm, respectively. Evidently, the α-Fe phase fraction increases with increasing powder sizes at the stoichiometric composition. The α-Fe phase is easily formed when the powder size is large, because of the low cooling rate of the atomization process compared with melt spinning or strip casting [9].

$Nd_{12}Fe_{82}B_6$ billets were fabricated using the SPS equipment to a powder size range of 25-38 μm, pre-compacted at 750°C, and then plastic deformed by die upsetting at 700, 800 and 900°C. Figs. 3(a)-(d) show the microstructures of the cross section of the perpendicular to die upsetting direction in pre-compacted and plastic-deformed billets, respectively. As shown in Fig. 3(a), many pores are observed before plastic deformation. The powder formed seems isotropic, and the densification is not perfect, because the Nd-rich phase quantity is very low; therefore, the pores at the particle boundaries could not be filled during

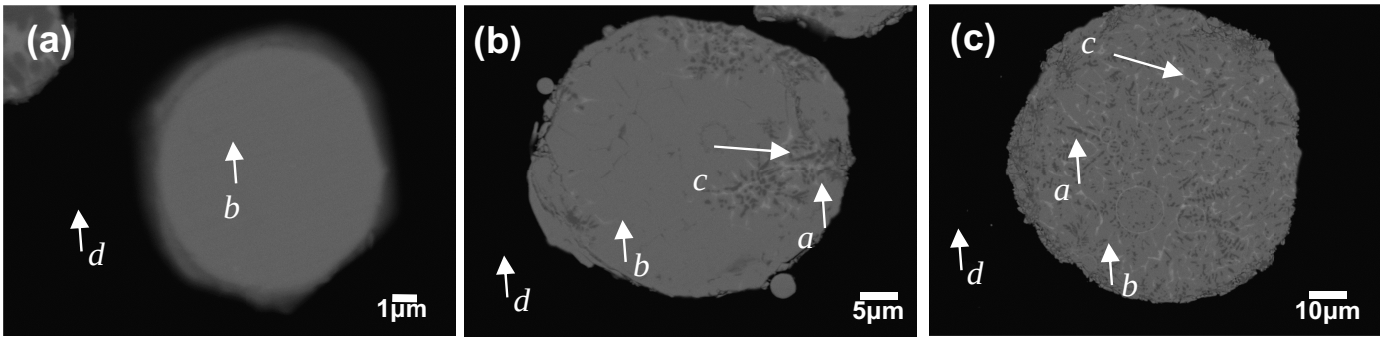

Fig. 2. Microstructures of gas atomized $Nd_{12}Fe_{82}B_6$ composition powder with powder size (a) 10 μm, (b) 40 μm, and (c) 70 μm. *a*: α-Fe (dark), *b*: $Nd_2Fe_{14}B$ (gray), *c*: Nd-rich (white) phase, and d: resin region

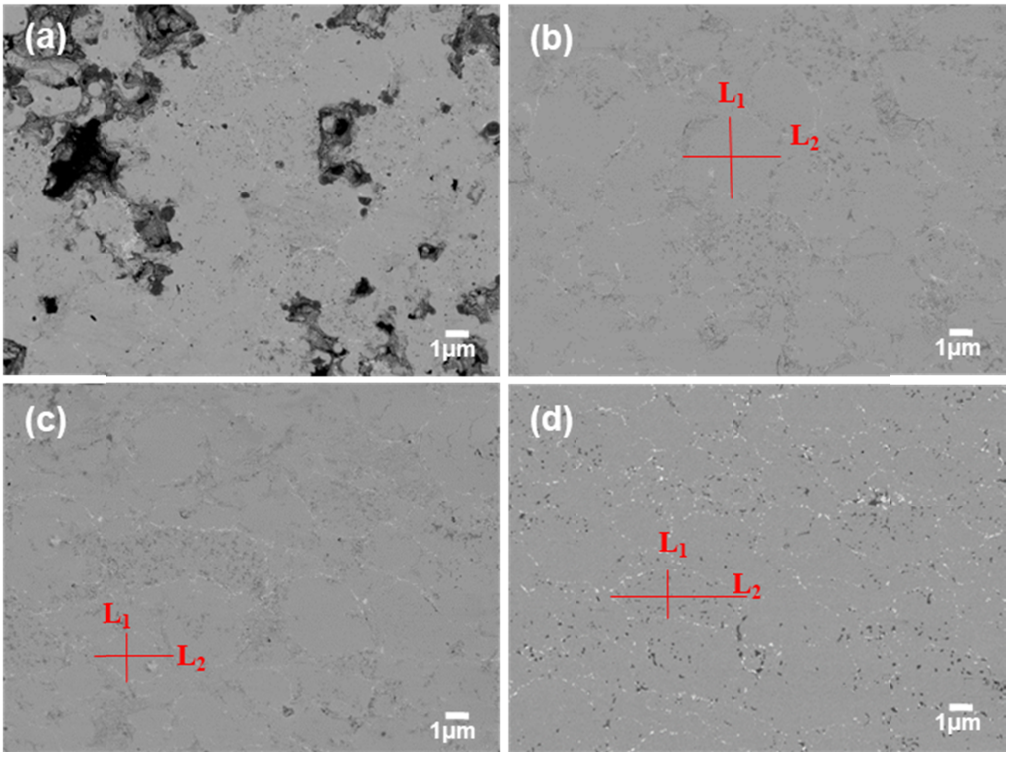

Fig. 3. Cross section of the perpendicular to die upsetting direction view for deformed patterns of SPS specimen at temperatures of (a) before deformation, (b) 700°C, (c) 800°C, and (d) 900°C (L_1: line of horizontal direction to die upsetting axis; L_2: line of parallel direction to die upsetting axis)

pre-compacting process. In contrast, the pores are eliminated after plastic deformation by die upsetting at high temperature (Fig. 3(b)-(d)). The apparent densities of the pre-compacted and plastic-deformed billets were 6.611 and 7.432 g/cm^3, respectively, and the relative densities of each with the $Nd_2Fe_{14}B$ phase (7.55 g/cm^3) were 88.6 and 98.4%, respectively. Plastic deformation seems to have occurred after the plastic deformation process, as indicated in Fig. 3(b)-(d).

To confirm the plastic deformability at high temperatures after die upsetting, the aspect ratio was calculated from the microstructure; Fig. 3(b)-(d) shows the result. The degree of plastic deformation increases with increasing plastic deformation temperature via L_1 (line horizontal to load axis) and L_2 (line perpendicular to load axis) lines (marked in red) in each figure. The Nd-rich phase located at the powder boundary and the $Nd_2Fe_{14}B$ matrix phase undergo more plastic deformation with increasing plastic deformation temperature. To confirm the plastic deformability quantitatively, the aspect ratio from the line of the horizontal direction relative to the die upsetting axis (L_1) and the line of the direction parallel to the die upsetting axis (L_2) was calculated for each sample; Fig. 4 shows the result. The aspect ratio increases from 1.3 to 2.4 after plastic deformation with an increase in temperature from 700 to 900°C. The aspect ratio increases only slightly (1 to 1.5) from before deformation to the plastic deformation temperature (800°C). When the temperature is above 800°C, the aspect ratio increases significantly. This can be attributed to the softening effect observed at higher temperatures, consistent with the high-temperature hardness test results shown in Fig. 1.

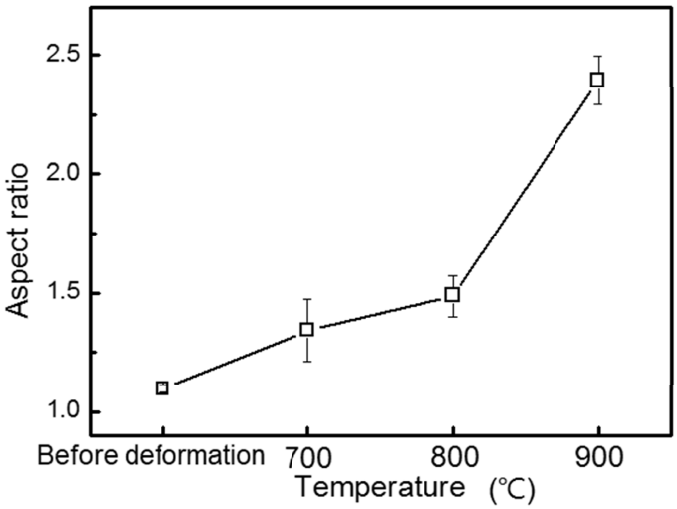

Fig. 4. Aspect ratio of the grains of $Nd_{12}Fe_{82}B_6$ with respect to deformation temperature

Fig. 5 shows the XRD peaks of the NdFeB alloy billets before and after plastic deformation. The diffraction pattern indicates a random alignment with the c-axis before deformation and after deformation at 700 and 800°C conditions. The peaks indicate that more high energy in the form of temperature or force is required for plastic deformation; an alignment with the c-axis is observed when the temperature is 900°C.

Since the peaks correspond to (004), (006), and (008) basal planes, which are planes of easy magnetization, it is necessary to determine the statistical distribution of the preferential planes.

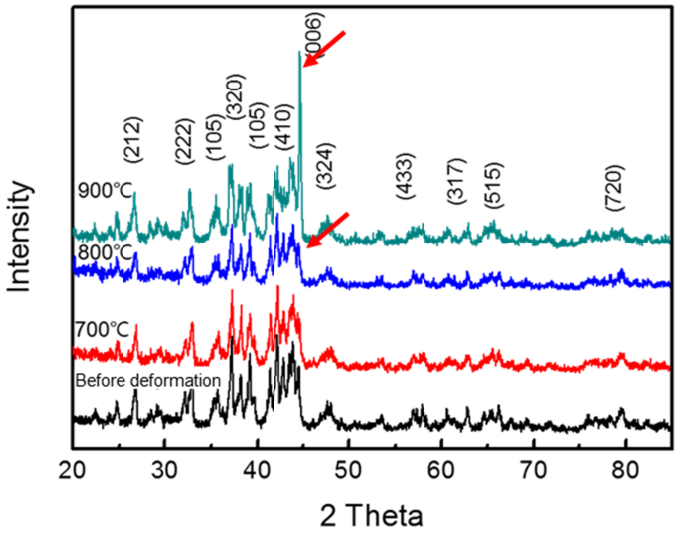

Fig. 5. Diffraction peaks of $Nd_{12}Fe_{82}B_6$ billets before and after plastic deformation with respect to deformation temperature

The orientation factor, which helps to quantitatively express c-axis alignment, can be calculated using Eq. (1) [10].

$$f = \frac{P - P_0}{1 - P_0} \; ; \; P = \frac{\sum I(0,0,l)}{\sum I(h,k,l)} \tag{1}$$

Here, f is the orientation factor, P is the fraction intensity of the (004), (006), and (008) planes, and P_0 is the value of P without any preferential orientation. Fig. 6 shows the calculated orientation factor with respect to temperature. The orientation factor increases with increasing temperature, similar to the trend in the aspect ratio (Fig. 4). The high-temperature hardness test results demonstrate that the orientation factor and aspect ratio are related to the softening effect in NdFeB alloys.

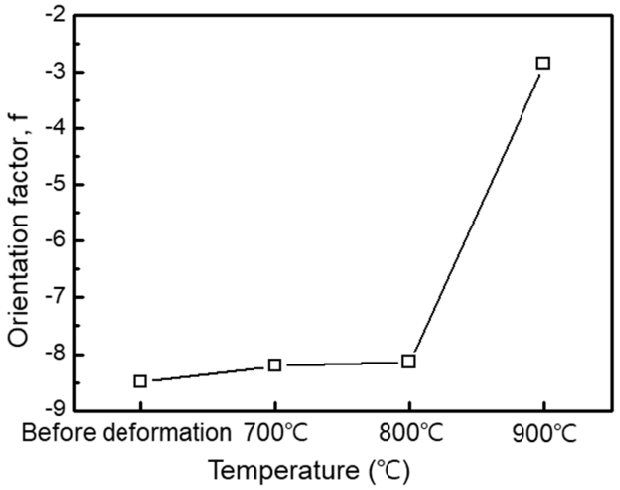

Fig. 6. Orientation factor of $Nd_{12}Fe_{82}B_6$ billets before and after plastic deformation with respect to deformation temperature

The magnetic properties of the $Nd_{12}Fe_{82}B$ alloys fabricated using atomized powders were quite poor, because of the lack of decoupling between the $Nd_2Fe_{14}B$ hard magnetic phases. This study focused on the plastic deformability between the $Nd_2Fe_{14}B$ hard magnetic phases; to enhance the magnetic properties, additional processes, such as doping or grain boundary diffusion process (GBDP), can be performed [11-13].

4. Conclusions

The plastic deformability of $Nd_{12}Fe_{82}B_6$ (stoichiometric composition) billets was studied through high-temperature hardness testing and spark plasma sintering of gas atomized powder. The softening occurred at high temperatures, thus confirming the possibility of plastic deformation of $Nd_{12}Fe_{82}B_6$ hard magnetic phases at high temperatures. After plastic deformation using the SPS process, the aspect ratio of the $Nd_{12}Fe_{82}B_6$ phase and the degree of c-axis alignment (represented by the orientation factor) increased with increasing temperature, particularly above 800°C. Although the magnetic properties were not as desired (because the magnet did not have any decoupling sources), they can be enhanced through additional processes such as doping or GBDP.

Acknowledgments

This research was supported by a grant from the project "Development of environment friendly pyrometallurgy process for high purity HREE and materialization" by the Korea Evaluation Institute of Industrial Technology (KEIT), Republic of Korea.

REFERENCES

[1] S.G. Yoon, Transfer. Super Strong Permanent Magnets, **1**, UUP, Ulsan (1999).
[2] J.G. Lee, J.H. Yu, Ceramist **17** (3), 50-60 (2014).
[3] H.Y. Yasuda, M. Kumano, T. Nagase, R. Kato, H. Shimizu, Scripta Materialia **65** (8), 743-746 (2011).
[4] S.F. Abbas, T.S. Kim, B.S. Kim, Metals and Magerials International. **24** (4), 860-868 (2018).
[5] B. Ma, V. Chandhok, E. Dulis, IEEE Transactions on Magnetics **23** (5), 2518-2520 (1987).
[6] J.H. Lee, J.Y. Cho, S.W. Nam, S.F. Abbas, K.M. Lim, T.S. Kim, Sci. Adv. Mater. **9** (10), 1859-1862 (2017).
[7] Y. Sakaguchi, T. Harada, T. Kuji, Mater. Sci. Eng. A **181**, 1232-1236 (1994).
[8] R.K. Mishra, J. Appl. Phys. **62** (3), 967-971 (1987).
[9] J.Y. Cho, S.F. Abbas, Y.H. Choa, T.S. Kim, Arch. Metall. Mater. **64** (2), 623-626 (2019).
[10] T.S. Chin, M.P. Hung, D.S. Tsai, K.F. Wu, W.C. Chang, J. Appl. Phys. **64** (10), 5531-5533 (1988).
[11] H. Nakamura, Scripta Materialia **154**, 273-276 (2018).
[12] H.W. Chang, Y.I. Lee, P.H. Liao, W.C. Chang, Scripta Materialia **146**, 222 (2018).
[13] Y.I. Lee, Y.J. Wong, H.W. Chang, W.C. Chang, J. Magnetism Magnetic Mater. **478**, 43-47 (2019).